69th International Astronautical Congress (IAC), Bremen, Germany, 1-5 October 2018.

IAC-18,C4,6,12,x46846

Trajectory and control systems design for a hovering mesopause probe

Dorian Hargarten[a]*, Josef Ettl[b], Karl W. Naumann[c]

[a] *Mobile Rocket Base, German Aerospace Research Center, Münchener Straße 20, D-82234 Weßling, Germany,* dorian.hargarten@dlr.de, [b]joset.ettl@dlr.de
[c] *BayernChemie GmbH, P.O. Box 1131, D-84454 Aschau am Inn, Germany,* karl.naumann@mbda-systems.de
* Corresponding Author

Abstract

Owing to the difficulty in reaching and maintaining the altitude of middle atmosphere layers such as the mesopause, performing in-situ experiments is typically limited in scope. This paper presents a novel approach to overcome both the altitude limitations of balloons and conventional aircraft as well as the limitations of ballistic sounding rocket flight profiles by employing a hovering probe. A throttleable rocket engine burning a storable monopropellant allows the probe to follow a constant-altitude trajectory and to perform science experiments and measurements during its burn phase. In this paper, the different development aspects required to successfully and safely perform such a mission are examined, focusing on trajectory optimization and trajectory and attitude control system aspects, while also presenting mission design and launch vehicle design. Parameter variation simulations are employed to demonstrate robustness of mission design and control algorithms against varying mission and vehicle parameters as well as perturbations. Given vehicle and engine parameters derived from preliminary designs and tests, flight performance simulations yield measurement distances on the order of 20 to 30 km while maintaining a target altitude between 80 and 90 km.

Keywords: atmospheric physics, throttleable, hovering, mesopause, gelled propellant

Acronyms/Abbreviations

PMWE: Polar Mesospheric Winter Echoes, an atmospheric phenomenon observed in the radar frequency range in the winter months at altitudes between 55 and 85 km
TWR: Thrust-to-Weight Ratio
PI: Proportional-Integral controller
PID: Proportional-Integral-Derivative controller

1. Introduction

The middle atmosphere is the subject of various studies trying to understand the dynamics therein. The altitude band is generously defined as 10 to 120 km [1], with special attention paid to the noctilucent clouds which appear in the mesopause at 80 to 90 km altitude [2].

Measurements of the middle atmosphere are typically performed by Radar (e.g. the Andenes MF Radar [3]) and Lidar devices (such as ALOMAR-RMR, [4]), but in-situ measurements are used to complement the former. On recent atmospheric physics missions, in-situ measurements were executed to study charged particles, neutral gas density and other aspects while passing through the target altitude band on a ballistic trajectory [5]. The two PMWE missions launched from Andenes, Norway, in April of 2018 are exemplary of this use case. PMWE 1 achieved an apogee altitude of 125.6 km, while PMWE 2 achieved an altitude of 121.4 km. The two payloads splashed down at a downrange distance of 68 and 62 km, respectively. Other ballistic sounding rocket missions achieved similar performance values, therefore, PMWE 1 and 2 are taken as reference for the development of the hovering probe.

Due to the ballistic trajectory, PMWE 1 and 2 passed through the mesopause quickly, spending less than 30 seconds within the target altitude band from 80 to 90 km. In that time frame, they traversed a horizontal distance over ground of around 5 km. The data is listed in Tab. 1, while the trajectories are displayed in Fig. 1.

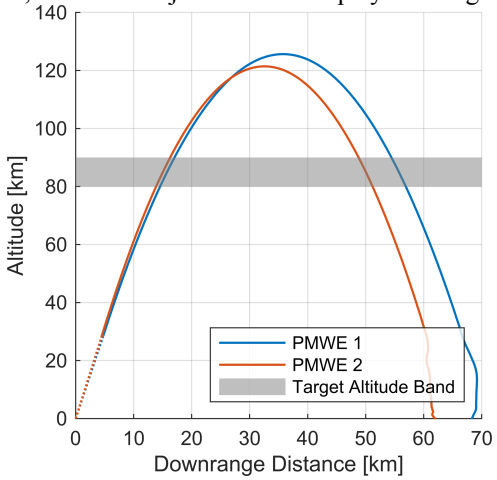

Fig. 1: PMWE 1 and 2 trajectory

	PMWE 1	PMWE 2
Apogee [km]	125.6	121.4
Distance traveled in target altitude range [km]	4.94	4.83
Downrange distance at splashdown [km]	68.4	62.0

Tab. 1: PMWE 1 and 2 performance results

It becomes evident that a ballistic trajectory is not well suited to study localized phenomena with limited vertical dimensions. The concept evaluated in this study is to hover at the target altitude while performing the experiments. The goal of this study is to maximize the distance travelled while at target altitude, the "measurement distance". The target altitude is set to 85 km but could be modified (within the first stage lifting capability) to accommodate different scientific objectives.

The concept of a hovering probe based on a gelled monopropellant engine has been described by P. Pinto in [6]. That paper also provides a preliminary hardware layout and mass breakdown. The following paper is based on the larger 300 kg vehicle described in Table 2, 3 and 4 in [6]. In addition, 50 kg of experiment payload was added, for a total vehicle mass of 350 kg, out of which 100 kg are consumable propellant.

The gelled propellant properties and research activities are described well in [7], while the results of long duration trial runs on a test bench engine fired at DLR Lampoldshausen and at BayernChemie are presented in [8]. The important results from those tests are that the prototype engines are able to run for 85 seconds without significant hardware degradation or temperature increase in the load-carrying structures. It is estimated that the trial engine could potentially run for much longer than 85 seconds. Also, the engine responded very quickly to thrust commands. [8]

This paper will describe the overall vehicle design, mission concept, and control system design for altitude and attitude control during the burn phase. The benefits of using such a hovering probe will be explored in the results section.

2. Material and methods

2.1. Thrust-controllable engines

The ability to throttle the engine over a wide thrust range is key to enable hovering probes, since firing the engine consumes the propellant and thereby reduces the total vehicle mass. The probe is required to hover until propellant depletion.

The authors of [9] describe means to achieve throttling with liquid propellant engines while [7] describes the same for gelled propellant engines. Some production liquid propellant engines offer a remarkably wide throttle range, for example Blue Origin's BE-3 achieves a range of 4.4:1 at a maximum sea-level thrust of 490 kN [10]. The Common Extensible Cryogenic Engine testbed, while not directly a production engine but based on the RL10, even achieved a throttle ratio of 13:1 [11]. Similarly wide throttle ranges can be achieved by gelled propellant engines, with prototype engines achieving ranges of up to 15:1 [7]. The gelled propellant engines developed within the German Gel Propulsion Technology Program are thrust-controllable, non restartable pressure-fed monopropellant engines producing a nominal thrust in the range of 2 to 20 kN. The various aspects of the program are presented in [7], while some application studies are provided in [6, 12–15].

2.2. Conditions in the mesopause

According to atmosphere model data such as the US Standard Atmosphere 1976, the ambient pressure at an altitude of 80 km is around 1 Pa, while the density amounts to about 18 mg/m^3 [16]. Therefore, the influence of aerodynamic effects can be neglected for the purposes of this study, and the flight is assumed to be exoatmospheric.

2.3. Means of attitude and thrust vector control

For attitude control of spacecraft with long operational time spans, a common technical solution features a cold or hot gas reaction control system combined with momentum wheels. Launch vehicles typically feature cold gas systems using nitrogen. During the burn phase, launch vehicles with liquid propellant engines often employ a movable engine mounted on a gimbal, whereas solid propellant rocket motors may feature a movable nozzle mounted on a flexible bearing. [17]

For the gelled propellant upper stage, both a cold gas reaction control system as well as a gimballed main engine are taken into consideration.

2.4. Vehicle design

The vehicle will consist of the upper stage (also referred to as the "probe") compromising the scientific payload, gelled propellant propulsion system as well as other necessary subsystems ("service system" for command and control, recovery system, separation system etc., [18]). The first stage will feature a conventional solid propellant rocket motor, e.g. the Improved Malemute. The first stage will use fins for aerodynamic stability. The fins will also be canted slightly to induce a roll, which helps reduce dispersions from thrust and aerodynamic asymmetry.

2.5. Mission concept

The vehicle will be launched from Andøya Space Center in Andenes, Norway. This launch facility also offers radar installations which can be used to complement the scientific in-situ measurements with

real-time ground-based measurements. The payload mass and launcher elevation should be chosen in such a way that the first stage apogee matches closely the target altitude. After first-stage burn out, the upper stage will not separate right away; instead it will coast until the ambient pressure has subsided sufficiently. This allows the vehicle to remain aerodynamically stable without requiring fins on the upper stage. The de-spin mechanism can be deployed before stage separation, that way it can be placed on the first stage and does not add to the upper stage mass. After stage separation, the upper stage will correct its attitude, and fire its engine to reach the target altitude. The effect of different initial apogee altitudes and launcher elevations on the science phase will be explored in section 4.2.

3. Theory and calculation

3.1. Vehicle Model

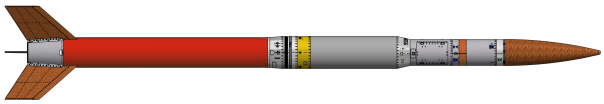

Fig. 2: Preliminary vehicle design

Since the successful long duration burn tests performed on test benches used the propellant variant GRP-006, this propellant is assumed to be used for the thrust controlled upper stage as well. It features a theoretical exhaust velocity of 2182 m/s and a density of 1.16 g/cm^3 [8]. The upper stage will contain 100 kg of propellant, with a dry weight of 250 kg. The maximum thrust of the flight-proven motor is around 6 kN [19], and preliminary simulations indicate that this motor fits well into the vehicle concept. The throttle-range is likely to be very wide (on the order of 10:1), while for the simulations presented in this paper, the range was (conservatively) assumed to be 6:1.

3.2. First stage trajectory

When launching an unguided sounding rocket, there exists a proportional relationship between launcher elevation and apogee altitude: the higher the elevation, the steeper the trajectory and hence the higher the apogee. On the contrary, a steeper ascent also correlates with a shorter downrange distance at splashdown as well as a lower horizontal velocity, which goes against the goal of maximizing the horizontal distance travelled at target altitude. If the first stage apogee doesn't match the target altitude, then the vehicle needs to burn propellant just to arrive at target altitude, and therefore less propellant is left for the science phase. It is intuitively understandable that the first stage apogee should match the target altitude as closely as possible.

3.3. Trajectory optimization

To maximize the distance travelled at target altitude, the impact of different upper stage pitch programs was investigated. Since the vehicle is supposed to maintain a constant altitude, varying the pitch angle also changes the overall thrust since the vertical thrust component always needs to counteract gravity. Pitching thereby also changes the horizontal acceleration. It is assumed for this analysis that the vehicle starts off at target altitude, and that it has a certain initial horizontal velocity imparted by the first stage.

The simplest pitch "program" would be to remain at a constant pitch angle throughout the burn phase. This would mean the engine would be throttled back due to the decreasing mass. The horizontal acceleration would remain constant as well.

Another possible pitch program would be to constantly fire the engine at maximum thrust, and reduce the pitch angle to maintain a constant altitude.

The last possibility for pitch programs are time-dependent pitch and thrust curves. The commanded pitch was chosen as a linear function of time with the parameters initial value and slope.

3.4. Altitude Controller

Since traveling along a constant-altitude trajectory is the key goal of this mission concept, the altitude controller performance is of particular prominence. When considering downleg-type trajectories where the vehicle falls from above target altitude, [20] and [21] elaborate that it is the most energy efficient (and hence fuel efficient) strategy to fire the engine at maximum thrust until target altitude is reached. In soft landing applications, this is also referred to as a "hoverslam" or "suicide burn" [22]. This leads to a minimum duration deceleration phase. If the engine is ignited earlier and fired at lower than maximum thrust, the deceleration phase is lengthened, the fuel consumption is increased, and the science phase is shortened.

For the inverse case, where the vehicle starts out below target altitude (upleg-type trajectories), it has been found that the fuel optimal trajectory is that which fires the engine at its minimum thrust setting until target altitude is reached. Coasting for longer and then firing the engine at above its minimum thrust setting increases fuel consumption and shortens the science phase.

3.4.1. Feedback Law

In his paper [21], J. Billingsley elaborates that for position control systems where the actuator produces a force acting on the plant, "conventional" proportional-integral-derivative (PID) controllers cannot achieve time-optimal behavior for different initial conditions, unless the controller parameters are tuned for each initial condition. The author then suggests using a cascading controller design, where the outer loop

calculates a commanded velocity based on a physical model of the plant. This calculation also includes the actuator limits, which in our case are maximum and minimum thrust. The inner loop consists of an aggressively tuned velocity controller.

This approach has been adapted to our case of a hovering rocket probe. Since propellant consumption changes the vehicle mass and hence the obtainable acceleration (at the actuator limits maximum or minimum thrust) is not constant anymore, further modifications are necessary and will be discussed below.

$$\ddot{x}_{const} = \begin{cases} \frac{F_{max}}{m} - g, x_e \geq 0 \\ \frac{F_{min}}{m} - g, x_e < 0 \end{cases} \quad (1)$$

$$x_e = x - x_c \quad (2)$$

Equation (1) calculates the desired, constant acceleration which depends on the engine thrust limits (F_{max} and F_{min}, respectively), the current vehicle mass (m) and the constant gravity acceleration (g). If the vehicle is above target altitude (x_c), then the altitude error (x_e) is positive ($x_e > 0$), and the goal is to fire at full thrust to decelerate as quickly as possible. If x_e is negative, then the goal is to fire at minimum thrust.

$$\dot{x}_c = x_e \cdot \sqrt{\frac{2\ddot{x}_{const}}{|x_e|}} \quad (3)$$

The commanded velocity is then calculated by solving equation (3). It is derived in [21], and it can be intuitively understood by assuming one starts at target altitude with zero velocity and then starts moving the vehicle with the constant acceleration $\ddot{x}_{const}$ until arriving at the current altitude error x_e.

The velocity error is then fed into a proportional controller:

$$F = -P \cdot (\dot{x} - \dot{x}_c) \quad (4)$$

If the vehicle starts falling from an apogee above target altitude, then at first the commanded velocity will be below the actual velocity. According to equation (4), the commanded thrust would be negative, and the engine remains switched off. At some point, the commanded velocity and the actual velocity cross, and the commanded thrust becomes positive. Once the thrust commands surpass the minimum thrust, the engine is ignited. The vehicle then travels downwards while firing at close to maximum thrust and arrives at target altitude with zero vertical velocity.

If the vehicle rises towards an apogee from below target altitude, then the commanded velocity will be positive. If the current velocity is higher than the commanded velocity, then the commanded thrust would be negative, and the engine would remain switched off. At some point before apogee, commanded and actual velocity will cross, and the once the commanded thrust surpasses the minimum thrust, the engine is ignited. The vehicle then travels upwards while firing at close to minimum thrust and arrives at target altitude with zero vertical velocity. The points of ignition are visible as a kink in the vertical velocity curves shown in Fig. 3.

The controller and vehicle behavior for these two scenarios is shown in Fig. 3.

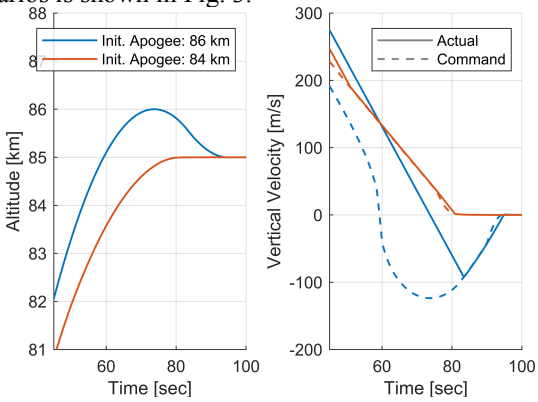

Fig. 3: Altitude, actual vertical velocity and commanded vertical velocity for an "undershoot" and an "overshoot" scenario

It is important to note that the approach from [21] assumes that the plant is capable of maintaining a constant acceleration at constant actuator output. Since the vehicle's mass decreases as the propellant is consumed, this is not the case for our study. On the downleg, the acceleration calculated by equation (1) increases as the mass decreases, since the maximum thrust and the other variables remain constant. This in turn leads to the commanded thrust increasing over time, which can be observed in the thrust curves shown in Fig. 7. The commanded thrust does, however, remain within vehicle limits. This means that the engine does not fire at full thrust the entire time of descent. This approach is therefore not perfectly fuel optimal, but it does work close to optimally for the different scenarios considered. On the upleg, however, this is problematic, since the required acceleration decreases below what is achievable at minimum thrust. This can be overcome by increasing the thrust used for equation (1) by e.g. 15 % over the minimum thrust, thereby ensuring that the resulting acceleration remains within vehicle limits. The percentage indirectly reflects the change of propellant mass fraction due to the amount of propellant consumed during target altitude approach – the longer the approach, the more propellant is consumed, and the higher the percentage should be. In the cases considered in this paper, 15 % suffices.

The feedback law from equation (4) is improved by introducing a linearized region around $x_e = 0$. This serves to reduce the feedback law steepness as described in [21]. Also, the control parameter P is scaled using the current gravity force acting on the vehicle. The goal of this gain scheduling is to reduce the influence of the

vehicle mass decrease on controller performance. The controller effectively commands a thrust-to-weight-ratio (TWR), which is then multiplied by the current vehicle gravity force to calculate the desired thrust. Lastly, a constant offset of $TWR_c = 1$ is added to the controller output, enabling the controller parameter P to be set at a lower value. Alternatively, a proportional-integral (PI) controller was evaluated but yielded difficulties related to integrator wind-up. These studies go beyond the scope of this paper.

3.5. Attitude control

As soon as the vehicle leaves the denser parts of the atmosphere, the aerodynamic stabilization provided by the first stage fins becomes ineffective. After deploying the de-spin mechanism, there might still be residual angular rates present. Before the upper stage engine can ignite its engine and commence the science phase, the vehicle's attitude needs to be set correctly. Also, during the burn phase, the vehicle's attitude needs to be controlled. To accomplish those points, the vehicle will feature an attitude control system. Roll control will be provided by a set of roll thrusters which use cold gas (Nitrogen is used typically). They are positioned in such a way that they produce torque only about the roll axis. Pitch and yaw control can be provided by either mounting the engine and nozzle on a movable gimbal, or by cold gas thrusters firing laterally.

The two different actuators are driven by PD controllers which were designed for robustness in disturbance rejection and reasonably fast performance following step commands.

The gimbal range is assumed to be +/- 2 degrees, while the maximum rate is assumed to be 20 degrees per second. The maximum cold gas thrust is assumed to be 10 N, with the lever arm for the pitch and yaw thrusters being around 1.5 m.

It is important to note that all attitude controllers considered above each acted on a single axis of rotation only. The control system design is not intended for coupled rotations such as if a residual roll coincides with a lateral rotation following stage separation.

4. Results and discussion

4.1. Best-case trajectory

Since the key goal of this study is to maximize the measurement distance, Fig. 4 compares the best-case trajectory of such a thrust-controllable upper stage with PMWE 1, a conventional ballistic sounding rocket. The first stage apogee is set precisely to the target altitude (85 km). The downrange distance travelled while within +/- 100 m of the target altitude is 30 km.

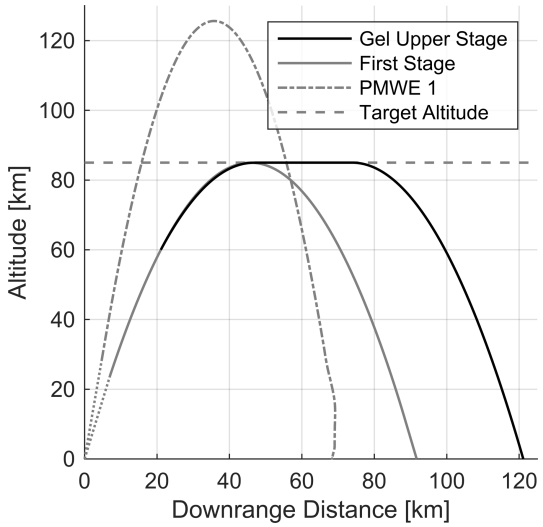

Fig. 4: Trajectory comparison with PMWE 1

4.2. Launcher elevation

If the launcher elevation is varied, then the first stage apogee varies as well – steeper elevations yield higher first stage apogee values and vice versa. As explained above, a first stage apogee "mismatch" reduces the amount of propellant left for the science phase, and the distance travelled at target altitude decreases. Fig. 5 shows the distance which is travelled at an altitude of 85 km +/- 100 m for various first stage apogee values. The peak occurs at a first stage apogee of 85 km.

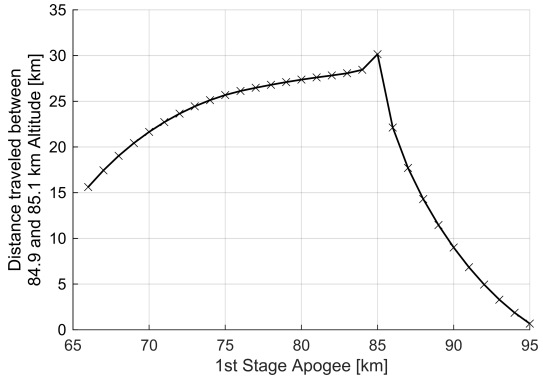

Fig. 5: Achievable Distance values for various first stage apogee values

It demonstrates that this decrease is much steeper for the "overshoot" scenarios (where the first stage apogee is above target altitude) than for the inverse case. This can be explained by "gravity losses": when the vehicle is traveling downwards towards target altitude, it needs to decelerate to arrive at target altitude with zero velocity. The higher the maximum engine thrust, the shorter the engine needs to fire at full thrust to decelerate. If the engine burn is shorter, so is the time that the engine is counteracting the gravity acceleration,

and therefore the amount of propellant consumed during deceleration is reduced as well. It has been investigated that the engine modelled so far with a maximum thrust of 6 kN is much better suited for "undershoot"-scenarios, because its maximum thrust-to-weight-ratio is low. A higher thrust engine would render a more symmetrical profile when compared with Fig. 5.

The distance and time spent for various values of launcher elevation are given in Tab. 2. It can be observed that lowering the launcher elevation significantly increases the splashdown distance. This is also demonstrated by Fig. 6.

Case:	Low elevation	Medium elevation	High elevation
First stage apogee [km]	70	79	85
Measurement distance [km]	21.7	27.1	30.2

Tab. 2: Performance data for thrust controllable upper stage

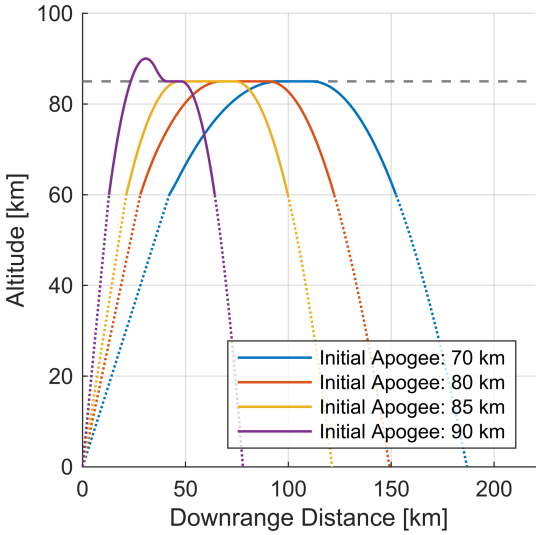

Fig. 6: Trajectory comparison for various first stage apogee values

4.3. *Thrust curves*

The output of the altitude controller described in section 3.4 is presented in Fig. 7.

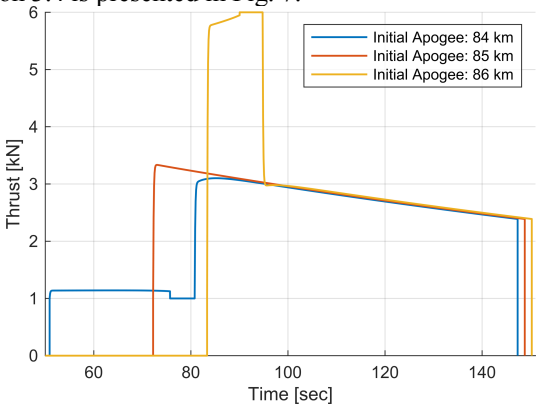

Fig. 7: Main engine thrust curves for various initial apogee values

It can be seen that for "undershoot"-scenarios, where the initial apogee lays below the target altitude, the engine is fired at close to minimum thrust until target altitude is reached, and then the engine thrust counteracts the gravity force. For the "overshoot"-scenarios, the engine fires at close to full thrust before arriving at target altitude.

4.4. *Pitch profile optimization*

Fig. 8 demonstrates that for a lower initial horizontal velocity, the measurement distance can be increased by pitching the vehicle further down towards horizontal. The term "pitch angle" is used here to refer to the angle the horizontal plane and the vehicle's longitudinal axis. Pitching down increases horizontal acceleration. A higher initial horizontal velocity requires a more upright attitude with a lower pitch angle, thereby producing less horizontal acceleration and instead using the propellant to coast longer.

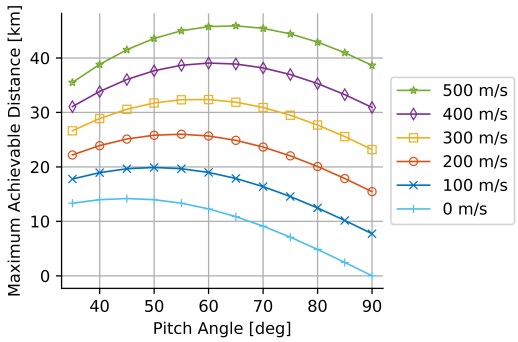

Fig. 8: Maximum science distance as a function of (time-invariant) pitch angle and initial horizontal velocity

If the engine is instead fired at full thrust, then the maximum measurement distance is much lower, as demonstrated by Fig. 9. The reason for this is that the

horizontal acceleration increases towards the end, without the vehicle being able to profit from the resultant higher velocity since the propellant is consumed much faster by firing at maximum thrust.

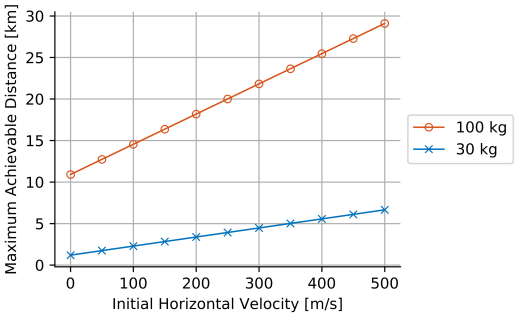

Fig. 9: Maximum science distance as a function of initial horizontal velocity and propellant mass if the constantly engine is fired at a maximum thrust of 6 kN during the science phase

The measurement distance can be increased even further by using a time-variant pitch angle. The best strategy is to first pitch down and accelerate horizontally, and then pitch up and coast (at a lower thrust and therefore longer coasting period). An example is displayed in Fig. 10. The vehicle starts with a horizontal distance of 300 m/s and a pitch angle of 33.65 degrees. It pitches upwards with a rate of 4.74 deg/s until it reaches a vertical attitude. It then remains vertical until the propellant is depleted.

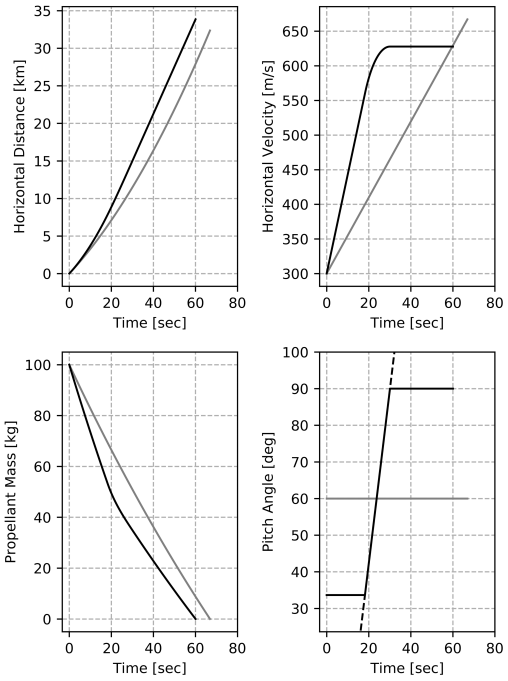

Fig. 10: Trajectory comparison between the best constant pitch angle (gray) and the best time-variant pitch profile (black).

The pitch profile parameters used for the simulation displayed in Fig. 10 were found using numerical optimization. The measurement distance is increased by 5 % compared to the best constant pitch profile, which was obtained at an angle of 60 degrees.

4.5. Attitude control results

Exemplary angular trajectories for step commands in the presence of a constant main engine thrust misalignment have been simulated for the case of the gimballed main engine and for the lateral control using cold gas thrusters. The thrust curve for an initial apogee of 86 km displayed in Fig. 7 was taken as a reference. The results are displayed in Fig. 11 and Fig. 12.

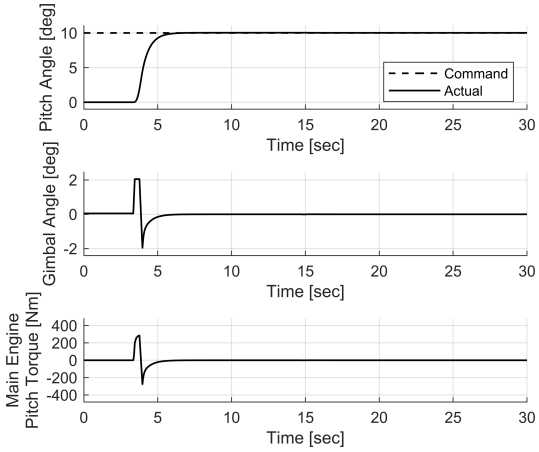

Fig. 11: Attitude control system response to pitch angle step command in the presence of a constant thrust misalignment of 0.05 degrees when using a gimballed main engine

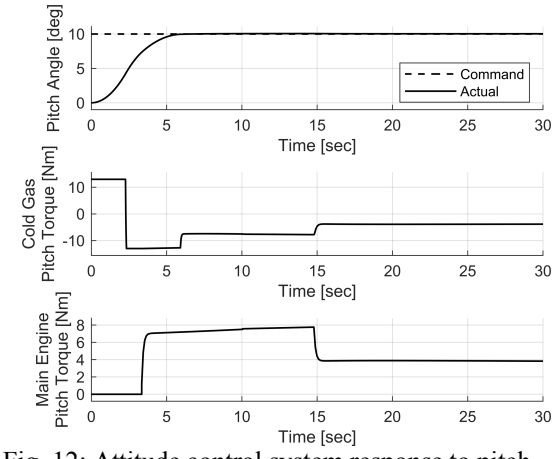

Fig. 12: Attitude control system response to pitch angle step command in the presence of a constant thrust misalignment of 0.05 degrees when using lateral cold gas thrusters

Due to the significant control torques produced by a gimballed engine, the control authority of the gimbal-

based control system is much higher than that based on 10 N cold gas thrusters. Therefore, the step response using the gimballed engine is much faster and features much less overshoot even in the presence of time-variant disturbances than in the case of cold gas thrusters. The control authority of the latter could be increased by using larger thrusters, but at a penalty of an increased consumption of cold gas. As an example, the gas consumption for the maneuver displayed in Fig. 12 (with a thrust misalignment of 0.05 degrees for a time span of 70 seconds) the cold gas consumed amounts to circa 0.38 kg.

5. Discussion

It has been shown in section 4.2 that the measurement distance reaches a maximum if the first stage apogee matches exactly the target altitude. Since the actual apogee is subject to dispersions, it is advisable to intentionally lower the first stage apogee to make sure that even in the case of an "overshoot", the measurement distance is not impacted too strongly.

Due to the limited control authority provided by lateral cold gas thrusters, and the significant mass of the cold gas consumed to compensate for disturbances such as thrust misalignments, the main engine construction and testing needs to verify that the actual thrust misalignments remain well under 0.1 degrees. If this cannot be guaranteed, then a movable engine needs to be implemented.

6. Conclusions

By comparing the results of our preliminary simulations with recent atmospheric physics missions, the benefit of a thrust controllable over ballistic sounding rockets becomes very clear. Instead of traveling just shy of 5 km while passing through a 10 km wide altitude band, the vehicle is able to remain within a 200 m band and travel a horizontal distance travelled of up to 30 km.

The engineering challenge in both construction of the propulsion module as well as implementation of the control systems should not be underestimated.

Acknowledgements

The author would like to thank the German Gel Propulsion Technology Working Group for their conducted work, as well as his colleagues at the German Aerospace Research Center (DLR).

References

[1] "Research Topics - Research - Leibniz-Institut für Atmosphärenphysik, Kühlungsborn," https://www.iap-kborn.de/en/research/research-topics/, [retrieved 17 September 2018].

[2] "Noctilucent Clouds (NLC) - Research - Leibniz-Institut für Atmosphärenphysik, Kühlungsborn," https://www.iap-kborn.de/en/research/department-optical-soundings-and-sounding-rockets/research-topics/noctilucent-clouds-nlc/, [retrieved 17 September 2018].

[3] "MF radars - Research - Leibniz-Institut für Atmosphärenphysik, Kühlungsborn," https://www.iap-kborn.de/en/research/department-radar-remote-sensing/instruments/mf-radars/, [retrieved 17 September 2018].

[4] "Temperature and wind soundings - Research - Leibniz-Institut für Atmosphärenphysik, Kühlungsborn," https://www.iap-kborn.de/en/research/department-optical-soundings-and-sounding-rockets/research-topics/temperature-and-wind-soundings/, [retrieved 17 September 2018].

[5] "PMWE - Forschung - Leibniz-Institut für Atmosphärenphysik, Kühlungsborn," https://www.iap-kborn.de/forschung/abteilung-optische-sondierungen-und-hoehenforschungsraketen/forschungsschwerpunkte/pmwe/, [retrieved 4 September 2018].

[6] Pinto, P. C., Naumann, K. W., Ramsel, J., Meyer, T., and Rest, S., "Stage concept for a hovering thermosphere probe vehicle with green,s afe and affordable gelled propellant rocket motors,".

[7] Ciezki, H. K., Kirchberger, C., Stiefel, A., Kroger, P., Caldas-Pinto, P., Ramsel, J., Naumann, K. W., Hürttlen, J., Schaller, U., Imiolek, A., and Weiser, V., "Overview on the German Gel Propulsion Technology Activities: Status 2017 and Outlook," 2017; 14 pages. doi: 10.13009/EUCASS2017-253.

[8] Pinto, P. C., Ramsel, J., Bauer, K., Risse, S., Naumann, K. W., Thumann, A., and Kurth, G., "Long Duration Test Runs of a Highly Throttleable Gelled Propellant Rocket Motor," *52nd AIAA/SAE/ASEE Joint Propulsion Conference,* American Institute of Aeronautics and Astronautics, Reston, Virginia, 07252016.

[9] Casiano, M. J., Hulka, J. R., and Yang, V., "Liquid-Propellant Rocket Engine Throttling: A Comprehensive Review," *Journal of Propulsion and Power*; Vol. 26, No. 5, 2010, pp. 897–923. doi: 10.2514/1.49791.

[10] "Blue Origin Tests New Engine in Simulated Suborbital Mission Profile – Parabolic Arc," http://www.parabolicarc.com/2013/12/03/blue-origin-tests-engine-simulated-suborbital-mission-profile/, [retrieved 17 September 2018].

[11] Brian Dunbar, "NASA Tests Engine Technology for Landing Astronauts on the Moon," https://www.nasa.gov/home/hqnews/2009/jan/HQ

_09-005_Cryo_engine_test.html, [retrieved 14 September 2018].

[12] Naumann, K. W., and Pinto, P. C., "Green, Controllable, Safe, Affordable and Mature Gelled Propellant Rocket Motor Technology for Space and Sub-Orbital Launchers," *2018 Joint Propulsion Conference,* American Institute of Aeronautics and Astronautics, Reston, Virginia, 07092018, p. 539.

[13] Naumann, K. W., Ciezki, H. K., Caldas-Pinto, P., Ramsel, J., Niedermaier, H., Thumann, A., and Kurth, G., "Green Gelled Propellant Throtteable Rocket Motors for Affordable and Safe Micro-Launchers," 2017; 14 pages. doi: 10.13009/EUCASS2017-154.

[14] Naumann, K. W., Ramsel, J., Schmid, K., Caldas-Pinto, P., Niedermaier, H., and Thumann, A., "Application of green propulsion systems using reocket motors and gas generators with gelled propellants,".

[15] Naumann, K. W., Ciezki, H. K., Caldas-Pinto, P., Ramsel, J., Niedermaier, H., and Rest, S., "A modular sounding rocket concept with green, safe and affordable gelled propellant rocket motorsw,".

[16] Carmichael, R., "A Table of the Standard Atmosphere to 86 km in SI units," http://www.pdas.com/atmosTable1SI.html, [retrieved 17 September 2018].

[17] Sutton, G. P., and Biblarz, O., *Rocket propulsion elements,* 7th edn., Wiley, New York, 2001.

[18] Kirchhartz, R., Hörschgen-Eggers, M., and Jung, W., "Sounding Rockets are unique Experimental Platforms," *69th International Astronautical Congress,* Bremen, Germany, October 1-5, 2018.

[19] Naumann, K. W., Ciezki, H. K., Stierle, R., Schmid, K., and Ramsel, J., "Rocket propulsion with gelled propellants for sounding rockets," *20th ESA Symposium on European Rocket and Balloon Programmes and Related Research 22 - 26 May 2011.*

[20] Meditch, J., "On the problem of optimal thrust programming for a lunar soft landing," *IEEE Transactions on Automatic Control*; Vol. 9, No. 4, 1964, pp. 477–484. doi: 10.1109/TAC.1964.1105758.

[21] J. Billingsley, "On the design of position control systems - Control Theory and Applications,".

[22] SpaceX, "Reusability," https://www.spacex.com/reusability-key-making-human-life-multi-planetary, [retrieved 17 September 2018].